Single molecule imaging of transcription dynamics, RNA localization and fate in T cells

M. Valeria Lattanzio[1,2], Nikolina Šoštarić[1,2,3], Nandhini Kanagasabesan[1,2], Branka Popović[1,2], Antonia Bradarić[1,2], Leyma Wardak[1,2], Aurélie Guislain[1,2], Philipp Savakis[4], Evelina Tutucci[4,#], and Monika C. Wolkers[1,2,#]

[1] Sanquin Blood Supply Foundation, Department of Research, T cell differentiation lab, Plesmanlaan 125, Amsterdam, The Netherlands, and Landsteiner Laboratory, Amsterdam Institute for Infection & Immunity, Cancer center Amsterdam-Cancer Immunology, Amsterdam UMC, University of Amsterdam, Meibergdreef 9, Amsterdam,

[2] Oncode Institute, Utrecht, The Netherlands

[3]Department of Bionanoscience, Kavli Institute of Nanoscience, Delft University of Technology, Van der Maasweg 9, 2629 HZ Delft, The Netherlands

[4]System Biology Lab, A-LIFE department, Amsterdam Institute of Molecular and Life Sciences (AIMMS), Vrije Universiteit Amsterdam, De Boelelaan 1085, NL-1081HV, Amsterdam, The Netherlands

#Corresponding authors. Email: evelina.tutucci@vu.nl | m.wolkers@sanquin.nl

Abstract

T cells are critical effector cells against infections and malignancies. To achieve this, they produce pro-inflammatory cytokines, including IFN-γ and TNF. Cytokine production is a tightly regulated process. The relative contribution of transcriptional and post-transcriptional regulation to mRNA expression is, however, unknown. We therefore implemented single-molecule FISH for primary human T cells (T-cell smFISH) to simultaneously quantify nascent RNA, mature mRNA levels and its localization with single-cell resolution. T-cell smFISH uncovered heterogeneous cytokine mRNA levels, with high cytokine producers displaying dual *IFNG*/*TNF* RNA transcription activity. Throughout activation, nuclear cytokine mRNAs accumulated, whereas cytoplasmic cytokine mRNA was degraded through translation-dependent decay. Lastly, T-cell smFISH uncovered cytokine-specific regulation by the RNA-binding protein HuR. Thus, T-cell smFISH provides novel insights in the intricate (post)-transcriptional processes in T cells.

Main Text

$CD8^+$ T cells play a crucial role in clearing infected and malignant cells. Upon target cell recognition, effector $CD8^+$ T cells undergo a substantial remodelling of their transcriptome and proteome (*1–4*). This remodelling allows for the rapid release of effector molecules such as granzymes and pro-inflammatory cytokines (*5*, *6*). Key pro-inflammatory cytokines are IFN-γ and TNF, which license T cells to kill their target cells (*7–9*).

Cytokine production is regulated at multiple molecular levels, including transcriptional and epigenetic mechanisms (*10*, *11*). Another important layer of gene expression control is post-transcriptional regulation (PTR), processes including - but not restricted to - RNA splicing, RNA transport, RNA stability, and translation control. The importance of PTR is evidenced by the fact that measured mRNA levels in T cells only mildly correlate with protein abundance (*4*), a highly conserved feature throughout evolution (*12*). For instance, antigen-experienced T cells contain ready-to-deploy cytokine mRNA, which is blocked through translational control, yet released from this block to serve as template for translation for rapid recall responses (*13*). Provided that cytokine overproduction induces immunopathology and autoimmunity, and that loss of production results in dysfunctional anti-tumor responses (*8*, *14*), it is of most importance to decipher how PTR processes control T cell function.

RNA binding proteins (RBPs) are key mediators of PTR that define the abundance of mRNA and protein in T cells (*6*, *15*, *16*). For instance, the RBP ELAVL1/HuR promotes early cytokine production of activated human $CD8^+$ T cells (*6*). In other cell types, HuR was shown to mediate pre-mRNA splicing, control poly-adenylation, regulate the nuclear export, and when located in the cytoplasm, promote mRNA stability and translation (*17–21*). Provided that RBP expression and their mode of action is cell-type specific (*22*, *23*), it remains to be uncovered how HuR promotes cytokine production in T cells.

The fate of an mRNA molecule is regulated at specific subcellular locations (*24*). In the nucleus RNA is transcribed, spliced, and modified. When translocated into the cytoplasm, translation can take place. Previous studies studying the life of mRNAs in T cells measured mRNA transcription, mRNA kinetics, and their subcellular localization by bulk RNA-sequencing (*25*, *26*). However, these studies lack single-cell resolution, which is pivotal when studying intrinsically highly heterogeneous T cell responses. Single-molecule fluorescence in situ hybridization (smFISH) provides such in-depth insights (*27*, *28*). smFISH can visualize and

quantify nascent cytokine mRNA at transcription sites, quantify mature mRNA and identify its subcellular localization, with single-cell resolution. Studies using smFISH in T cells (*29*, *30*) employed standard smFISH pipelines that were developed for adherent cells (*31*, *32*). Because these pipelines are not geared towards the small cell size and round morphology of T cells, they fail to unequivocally call the subcellular localization of transcripts. To overcome this limitation, we developed T-cell smFISH, a new analysis pipeline that precisely localizes nuclear and cytoplasmic mRNA for the investigation of (post)-transcriptional mechanisms in T cells. Using this pipeline, we achieved unprecedented depth of analyzing the fate of mRNA in T cells, here exemplified for cytokine mRNAs.

Quantifying cytokine mRNA in primary T cells with 3D single-molecule resolution

To quantify cytokine mRNAs in human T cells, we first optimized the smFISH hybridization and analysis protocol (*see Materials and Method*s). We generated effector T cells (Teff) that can rapidly respond to recall responses, by activating human blood-derived $CD8^+$ T cells for 72 h with α-CD3/α-CD28, followed by a 7-day of rest. Teff cells were subsequently restimulated with α-CD3/α-CD28, fixed, and simultaneously probed for *IFNG* and *TNF* mRNA by two-color smFISH (**Fig 1A**) (*28*, *33*). Z-stacks were acquired every 200 nm with a high-numerical aperture objective coupled to a wide-field fluorescence microscope to encompass the entire cell thickness, and to precisely identify the *x*, *y*, *z* position of an mRNA (*34*). T cell shape and outline were deduced from auto-fluorescence in the probe channel and from differential interference contrast images (DIC; **Suppl. Fig. 1A**). DAPI was used for nuclear staining (**Suppl. Fig. 1A**). To accommodate for the small and compact structure of T cells, T-cell smFISH pipeline was developed to localize individual cytokine mRNA molecules with subcellular resolution, by combining FISH-quant (*32*) for RNA quantification, filtering for cell selection, and Cell-Pose (*35*) for 3D mask reconstruction (**Suppl. Fig. 1B, Movie S1-S2;** https://github.com/nikolinasostaric/T-cell_smFISH). The T-cell smFISH pipeline achieved 98% accuracy, as defined by manual analysis of 100 randomly chosen mRNAs. T-cell smFISH thus allowed us to elucidate the expression of cytokine transcripts upon T cell activation with single-cell and subcellular resolution.

T-cell smFISH uncovers cytokine-specific transcription activity

Having established T-cell smFISH, we studied the cytokine mRNA dynamics during T cell activation with α-CD3/α-CD28. The key effector cytokines IFN-γ and TNF are produced early after T cell activation, yet with distinct kinetics (*36*, *37*). To uncover the underlying mechanism,

we measured nascent RNA and the subcellular distribution of mature mRNA (**Fig. 1C**), and we compared that to cytokine protein levels.

We first focused on nascent cytokine RNAs. Resting Teff cells (t=0h) were devoid of active transcription sites (TsX) for *IFNG* (**Fig. 1D, Suppl. Fig. 1C**). At 1 h of activation, however, 2% Teff cells expressed nascent *IFNG* mRNA with a median of 12 nascent RNAs per TsX (**Fig. 1D; Suppl. Fig. 1C-1D**). At 3 h of activation, active TsX peaked with 8%**,** with a median of 3 nascent *IFNG* RNAs per TsX, and this level of nascent RNA was maintained up to 6 h of activation (**Fig. 1D, Suppl. Fig. 1C-1D**). Of note, even though at 1 h of activation we observed bi-allelic transcription in 45% of the *IFNG*-transcribing cells, at later time points monoallelic *IFNG* transcription dominated (**Suppl. Fig. 1C**).

In contrast to *IFNG,* nascent *TNF* RNA is already detected in 1% of resting Teff cells with a median of 5 nascent RNA molecules per TsX (**Fig. 1D, Suppl. Fig. 1C-1D**). At 1h of stimulation, nascent *TNF* peaked with 13 nascent RNA per TsX, and dropped and stabilized at 2h with 6 molecules on average per cell (**Fig. 1D, Suppl. Fig. 1C-1D**). Intriguingly, this drop did not result from fewer active TsX for *TNF*. Furthermore, bi-allelic transcription was observed in 56% of the TNF-transcribing cells until 3 h of activation, and mono-allelic transcription was only more prevalent at later time points (**Suppl. Fig. 1C**). Thus, nascent *IFNG* and *TNF* RNA display different kinetics, with *IFNG* requiring T cell activation for *de novo* synthesis, and *TNF* already being active in resting Teff cells. *IFNG* transcription relies more on mono-allelic transcription, whereas *TNF* transcription also employs bi-allelic synthesis during early T cell activation.

Cytokine-specific kinetics of mRNA and protein expression during T cell activation

We next quantified mature *TNF* and *IFNG* mRNA. Even though nascent *IFNG* RNA was undetectable in resting Teff cells, 36% expressed low but detectable levels of mature *IFNG* mRNA, and 28% expressed mature *TNF* mRNA (each a median of 1 molecule/cell; **Fig.1E, Suppl. Fig. 1E**). At 1 h of stimulation, 77% T cells expressed mature *IFNG* and 74% expressed *TNF* mRNA (median of 4 and 13 molecules/cell, respectively; **Suppl. Fig. 1E-F**). Notably, with 1-200 *IFNG* and *TNF* mRNA molecules/cell, a high inter-cellular variability was observed in all three donors, at all time points measured (**Fig. 1E; Suppl. Fig. 1F)**. Yet, whereas a subset of Teff cells maintained high levels of mature *IFNG* mRNA throughout T cell activation (>100

molecules/cell; **Fig 1E**), the levels of mature *TNF* mRNA rapidly declined below 100 molecules/cell from 2 h of activation onwards (**Fig. 1E**).

Also the cytokine production displayed high intercellular and inter-donor heterogeneity (**Fig. 1F**). Following the expression patterns of mature mRNA, IFN-γ protein production peaked at 2 h of activation with a maximum of 10% of Teff cells and remained stable thereafter (**Fig. 1F**). Yet, IFN-γ protein levels per cell showed high inter-cellular variability and peaked at 4h post stimulation, as defined by median fluorescence intensity (**Fig. 1G).** Conversely, and in line with higher mature *TNF* mRNA levels at 1h of activation (**Fig. 1E**), TNF protein production peaked at 2-3 h of activation with 12% TNF-producing Teff cells, and rapidly declined thereafter (**Fig. 1F**). Yet, the protein production per cell remained constant throughout (**Fig.1G**). Combined, these data show that the protein production kinetics of IFN-γ and TNF follow the cytokine mRNA kinetics.

Dual cytokine mRNA-expressing Teff cells dominate the immune response

Dual cytokine producers are more potent effector T cells than single cytokine producers (*37*, *38*). We therefore questioned how single (SP) and double positive (DP) cytokine mRNA expressors (**Movie S1**) contribute to the observed high variability of cytokine mRNA expression. The number of nascent *IFNG* RNA per TsX was higher in DP Teff cells, but not of the nascent *TNF* (**Fig. 2A**). Yet, the percentage of active TsX was substantially higher in DP cytokine RNA-expressing Teff cells, which was observed at all time points **(Suppl. Fig. 2A**). In addition, DP T cells displayed more bi-allelic transcription for both cytokines (**Suppl. Fig. 2A**). Higher transcriptional activity in DP T cells also resulted in more mature cytokine mRNA (**Fig. 2B, C**). Upon T cell activation DP T cells expressed substantially higher percentages and numbers of mature *IFNG* mRNA/cell at all time points measured and mature *TNF* mRNA at early T cell activation time points (1-3 h) compared to SP T cells (**Fig. 2B, C)**. Not only mRNA, but also the percentage of protein-producing Teff and protein production/cell was higher in DP cytokine producers (**Fig. 2D, Suppl. Fig. 2B**). In conclusion, Teff cells with active TsX for both *IFNG* and *TNF* contain more mature cytokine mRNA. Furthermore, DP cytokine producers dominate the cytokine production kinetics upon T cell activation and contribute to the observed high inter-cellular heterogeneity of cytokine production.

Differential subcellular distribution of *IFNG* and *TNF* mRNA

Mature mRNA can only serve as template for translation when located in the cytoplasm. Therefore, we next investigated the subcellular distribution of *IFNG* and *TNF* mRNA during activation with T-cell smFISH (**Suppl. Fig. 3A**). In resting Teff cells, the vast majority of the little mature *IFNG* mRNA and *TNF* mRNA present was in the nucleus (**Fig. 3A, Suppl. Fig. 3A - top panel**). However, T cell activation rapidly shifted the distribution of mature *IFNG* mRNA to the cytoplasm (**Fig. 3A).** Yet, from 2 h of activation onwards, the *IFNG* mRNA was equally distributed between nucleus and cytoplasm (**Fig. 3A).** *TNF* mRNA was more prevalent in the nucleus throughout and was with 75% most apparent at the peak of its expression, i.e. at 1 h of T cell activation (**Fig. 3A, Suppl. Fig. 3A**). Thus, mature *IFNG* and *TNF* mRNAs differentially distribute between nucleus and cytoplasm in activated Teff cells.

Translation-dependent decay controls cytokine mRNA levels upon T cell activation

The unexpectedly high levels of mature cytokine mRNA in the nucleus prompted us to question how *de novo* transcription and translation contributed to the subcellular distribution. We therefore activated Teff cells for 2h and in the 2nd blocked *de novo* transcription with Actinomycin D (ActD) or translation with Harringtonine (Harr) (**Fig. 3B**). As expected, Harr treatment reduced both the overall translation as defined by puromycin incorporation, and the cytokine production (**Suppl. Fig. 3B, C**). Likewise, T-cell smFISH analysis showed that ActD almost completely blocked the presence of nascent RNA (**Fig. 3C**). ActD treatment also reduced the numbers of measured mature *IFNG* mRNA molecules/cell by 5-fold (**Fig. 3D**). Intriguingly, mature *TNF* mRNA expression was much less affected by ActD treatment (**Fig. 3D)**, indicating that the production boost of *TNF* mRNA during the first hour of T cell activation (**Fig. 1E**) suffices to maintain high levels of mature *TNF* mRNA expression during the 2nd hour of activation.

Notably, blocking translation with Harr increased the numbers of mature cytokine mRNA/cell compared to control (**Fig. 3D)**, indicating a feedback mechanism from translation to the overall mRNA expression. T-cell smFISH analysis uncovered that Harr treatment primarily increased the cytoplasmic *IFNG* mRNA and *TNF* mRNA (**Fig. 3E**). To determine whether this cytoplasmic accumulation upon Harr treatment resulted from translation-dependent mRNA decay, we simultaneously blocked translation and transcription and measured cytokine mRNA by qRT-PCR. ActD treatment alone reduced the overall cytokine mRNA levels by 60% compared to control (**Fig. 3F**), however, this reduction had little effect on the protein output (**Suppl. Fig. 3D, E**). In contrast, ActD/Harr treatment combined substantially reduced the

protein production (**Suppl. Fig. 3D, E)**. Yet, the expression levels for *IFNG* and *TNF* mRNA increased by 30% in ActD/Harr-treated Teff cells compared to Act treatment alone, and this increase was not observed for *IL2* mRNA (**Fig. 3F)**. Combined, the T-cell smFISH pipeline uncovered with single-cell resolution that translation regulates the cytoplasmic *IFNG* and *TNF* mRNA levels. Furthermore, *IFNG* and *TNF* mRNA - but not *IL2* mRNA- are subject to translation-dependent decay.

HuR differentially controls *IFNG* and *TNF* mRNA expression and cytokine production

Having established the cytokine mRNA expression kinetics and distribution in Teff cells, we questioned how RNA-binding proteins such as HuR regulate the fate of cytokine mRNA. HuR protein expression increased during the 2 h of T cell activation, however, HuR interacted with *IFNG* and *TNF* mRNA only at 1 h post-stimulation, and not at 2h post-stimulation, as determined by RNA-immunoprecipitation (RIP)-qRT-PCR (**Suppl. Fig. 4 A, B**). To study its role on cytokines, we depleted HuR from Teff cells by CRISPR-Cas9 gene editing (**Suppl. Fig. 4C)**. As previously reported (*6*), HuR-KO Teff produced less IFN-γ and TNF protein during the first 2h of activation, both in terms of percentage and protein production/cell **(Fig. 4A-B)**. Notably, without resulting in detectable protein production, T-cell smFISH analysis uncovered opposite effects on mRNA levels (**Fig. 4C-4D)**. Resting HuR-KO Teff cells already contained more *IFNG* mRNA expressing cells (**Suppl. Fig. 4D)**, and the median mRNA molecules/cell increased from 3 to 10 for *IFNG*, and from 5 to 9 for *TNF* (**Fig. 4D)**. At 1h of stimulation, the percentage of mRNA-expressing Teff cells and number of cytokine molecules/cell was also higher in HuR-KO (**Fig. 4D, Suppl. Fig. 4D).** Only at 2 h activation, numbers of cytokine mRNAs/cell dropped below those of control Teff cells (**Fig. 4D)**.

To determine whether the higher cytokine mRNA levels observed in HuR-KO Teff cells resulted from increased transcription, we studied the number of nascent RNA. Resting HuR-KO Teff cells contained 8 nascent *IFNG* RNA/cell compared to 5 nascent *IFNG* RNA/cell in control T cells, and this slight increase was lost by 2h post activation (**Fig. 4E**). In contrast, nascent *TNF* RNA remained unaffected by HuR depletion at all time points (**Fig. 4E)**. Thus, despite that HuR-KO T cells produce less cytokine during early activation, mature mRNAs accumulate, and transcription may only partly contribute to this accumulation.

HuR deletion affects the cellular distribution of *IFNG* and *TNF* mRNA

Because higher cytokine mRNA levels in HuR-KO cells did not result in higher but lower protein production, we questioned whether HuR depletion affected the subcellular mRNA distribution. T-cell smFISH analysis uncovered that resting HuR-KO Teff cells expressed significantly more cytoplasmic *IFNG* and *TNF* mRNA molecules than control Teff cells (**Fig. 5A**). HuR-KO Teff cells also contained slightly more nuclear *TNF* mRNA (**Fig. 5A**). Upon 1h activation, both cytokine mRNAs were slightly increased in both subcellular compartments, which was reversed at 2 h of T cell activation (**Fig. 5A**). When we determined the relative distribution of cytokine mRNA within each individual Teff cell, we found that resting HuR-KO T cells contain more *IFNG* mRNA in the cytoplasm, which drops at 1h but is reverted at 2h post-stimulation (**Fig. 5B)**. In contrast, *TNF* mRNA is slightly more nuclear at 0h and 1h activation in HuR-KO cells compared to control cells, and this effect is lost at 2h activation when HuR also loses its interaction with cytokine mRNAs (**Fig. 5B, Suppl. Fig. 4B**). Hence, HuR deletion influences the subcellular localization of cytokine mRNAs in a time-dependent manner.

HuR regulates the polyadenylation of *TNF* mRNA

Lastly, we aimed to decipher how HuR regulates cytokine RNA. HuR can stabilize its target mRNAs (*39*, *40*). However, measuring mRNA decay in T cells activated for 1h, and then treated for an additional 1-2h with ActD showed no differences in overall mRNA levels or RNA decay rates between HuR-KO and control Teff cells (**Fig. 5C**). Thus, HuR does not appear to regulate cytokine mRNA stability.

HuR can act as splicing factor (*18*, *41*). Yet, irrespective of the nuclear *IFNG* mRNA accumulation (**Fig. 5B**), no overt differences of intron-exon junctions were found between HuR-KO and control Teff cells (**Suppl. Fig. 5A)**. Additionally, even though splicing is considered a key event for *TNF* (*42*, *43*), HuR deletion has only limited- if any- effect on *TNF* splicing (**Suppl. Fig. 5A),** indicating that HuR is not essential for *IFNG* and *TNF* RNA splicing in T cells.

HuR can also regulate polyadenylation (*17*, *20*). However, we found no changes in the poly(A) tail profile of *IFNG* mRNA in HuR KO cells at 1h of T cell activation (**Fig 5D, Suppl. Fig 5B**). In sharp contrast, HuR deficiency substantially impaired the poly(A) tail of *TNF* mRNA (**Fig 5D, Suppl. Fig 5B**). Thus, HuR employs cytokine-specific regulatory mechanisms to control

the fate of mRNA, and ultimately the protein expression of these two key pro-inflammatory cytokines.

Discussion

In this study, we present the T-cell smFISH pipeline to simultaneously quantify nascent and mature cytokine mRNAs and their subcellular distribution. Importantly, this three-dimensional analysis of RNA expression with single-molecule and single-cell resolution can provide unprecedented insights in the regulation of cytokine production and the activity of RNA binding proteins in T cells, as we showcased for HuR.

Even though most activated Teff cells express cytokine mRNAs, they display a two order of magnitude difference in mRNA and protein expression. Within the highly heterogenous T cell responses, cytokine production upon T cell activation primarily originates from Teff cells that transcribe both cytokine mRNAs simultaneously, suggesting that this superior cytokine production by DP cells is cell-intrinsic. Whereas the underlying mechanism is yet to be uncovered, it is tempting to speculate that DP cells produce more cytokines because of 1) an open chromatin structure at the cytokine loci or their respective regulators, 2) high expression of cytokine-driving transcription factors, or 3) more responsive signaling cascades in response to T cell activation. T-cell smFISH may help uncover the underlying mechanisms.

The subcellular localization of cytokine mRNA dictates the amount of cytokine production. Indeed, T-cell smFISH uncovered that nuclear accumulation of *IFNG* and *TNF* mRNA, suggesting that nuclear retention (*44*) regulates the availability of cytokine mRNAs for translation. In addition, nuclear retention of *TNF* mRNA may support its efficient splicing as previously suggested (*42*, *43*). We here uncovered that translation-dependent decay (*45*) contributes to the lower cytoplasmic mRNA levels we measured, a feature that appeared transcript-specific, as *IL2* mRNA was resistant.

T-cell smFISH also provides novel insights in the mode of action of RBPs. HuR deficiency resulted in increased levels of *IFNG* and *TNF* mRNA, yet with lower protein production. Of note, smFISH probes can detect mature and pre-spliced RNA (*27*, *32*). However, splicing was not affected in HuR KO T cells. Intriguingly, T-cell smFISH revealed cytokine-specific regulation. HuR deficiency slightly altered the transcription of *IFNG* mRNA, but not that of

TNF mRNA. In turn, HuR is required for the polyadenylation of *TNF*, but not of *IFNG*. Polyadenylation can modulate mRNA stability (*46*), but mRNA stability was not altered for *TNF*. HuR can also promote alternative poly-adenylation and compete with the PolyA cleavage factor (*17*, *47*). Whether this induces the observed impaired translation of TNF is however yet to be determined. *IFNG* mRNA does not depend on HuR for splicing or polyadenylation. Therefore, HuR may regulate the nuclear export of *IFNG* mRNA during early T cell activation, as previously described for other target mRNAs (*48*, *49*). Irrespective of its exact mode of action on *IFNG* mRNA, our data highlight that HuR's activity is target-specific, as was previously reported for other RBPs (*23*, *50*).

In summary, T-cell smFISH is a sensitive and quantitative tool with single-cell, single- molecule resolution for deciphering post-transcriptional regulation. We uncovered that differential mechanisms govern *IFNG* and *TNF* mRNA kinetics and showcased the contribution of HuR in regulating T cell effector function. We propose T-cell smFISH as a powerful tool to uncover molecular mechanisms underlying dysregulated cytokine production, such as impaired production upon chronic stimulation (*51*) or excessive production in immunopathology (*14*, *52*, *53*). The custom-made T-cell smFISH pipeline we present here should support further studies on RNA expression and RBP-mediated regulation that define T cell function.

References

1. K. Araki, M. Morita, A. G. Bederman, B. T. Konieczny, H. T. Kissick, N. Sonenberg, R. Ahmed, Translation is actively regulated during the differentiation of CD8 + effector T cells. *Nat Immunol* **18**, 1046–1057 (2017).

2. T. Wolf, W. Jin, G. Zoppi, I. A. Vogel, M. Akhmedov, C. K. E. Bleck, T. Beltraminelli, J. C. Rieckmann, N. J. Ramirez, M. Benevento, S. Notarbartolo, D. Bumann, F. Meissner, B. Grimbacher, M. Mann, A. Lanzavecchia, F. Sallusto, I. Kwee, R. Geiger, Dynamics in protein translation sustaining T cell preparedness. *Nat Immunol* **21**, 927–937 (2020).

3. R. Rak, M. Polonsky, I. Eizenberg-Magar, Y. Mo, Y. Sakaguchi, O. Mizrahi, A. Nachshon, S. Reich-Zeliger, N. Stern-Ginossar, O. Dahan, T. Suzuki, N. Friedman, Y. Pilpel, Dynamic changes in tRNA modifications and abundance during T cell activation. *Proc Natl Acad Sci U S A* **118**, e2106556118 (2021).

4. B. P. Nicolet, M. C. Wolkers, The relationship of mRNA with protein expression in CD8+ T cells associates with gene class and gene characteristics. *PLoS One 17***.10,** e0276294 (2022).

5. F. Salerno, N. A. Paolini, R. Stark, M. Von Lindern, M. C. Wolkers, Distinct PKC-mediated posttranscriptional events set cytokine production kinetics in CD8+ T cells. *Proc Natl Acad Sci U S A* **114**, 9677–9682 (2017).

6. B. Popović, B. P. Nicolet, A. Guislain, S. Engels, A. P. Jurgens, N. Paravinja, J. J. Freen-van Heeren, F. P. J. van Alphen, M. van den Biggelaar, F. Salerno, M. C. Wolkers, Time-dependent regulation of cytokine production by RNA binding proteins defines T cell effector function. *Cell Rep* **42.5**, 112419 (2023).

7. H. Ikeda, L. J. Old, R. D. Schreiber, The roles of IFN in protection against tumor development and cancer immunoediting. *Cytokine & growth factor reviews*, ***13.*****2**, 95-109 (2002).

8. B. Zhang, T. Karrison, D. A. Rowley, H. Schreiber, IFN-γ- and TNF-dependent bystander eradication of antigen-loss variants in established mouse cancers. *Journal of Clinical Investigation* **118**, 1398–1404 (2008).

9. C. F. Nathan, H. W. Murray, I. E. Wlebe, B. Y. Rubin, Identification of interferon-gamma as the lymphokine that activates human macrophage oxidative metabolism and antimicrobial activity. *Journal of Experimental Medicine* **158**, 670–689 (1983).

10. J. M. Conley, M. P. Gallagher, L. J. Berg, T cells and gene regulation: The switching on and turning up of genes after T cell receptor stimulation in CD8 T cells. *Front Immunol* **7**, 182769 (2016).

11. A. N. Henning, R. Roychoudhuri, N. P. Restifo Epigenetic control of CD8+ T cell differentiation. *Nature Reviews Immunology*, *18*(5), 340-356 (2018).

12. B. Schwanhüusser, D. Busse, N. Li, G. Dittmar, J. Schuchhardt, J. Wolf, W. Chen, M. Selbach, Global quantification of mammalian gene expression control. *Nature 2011 473:7347* **473**, 337–342 (2011).

13. F. Salerno, S. Engels, M. van den Biggelaar, F. P. J. van Alphen, A. Guislain, W. Zhao, D. L. Hodge, S. E. Bell, J. P. Medema, M. von Lindern, M. Turner, H. A. Young, M. C. Wolkers, Translational repression of pre-formed cytokine-encoding mRNA prevents chronic activation of memory T cells. *Nat Immunol* **19**, 828–837 (2018).

14. R. Karki, B. R. Sharma, S. Tuladhar, E. P. Williams, L. Zalduondo, P. Samir, M. Zheng, B. Sundaram, B. Banoth, R. K. S. Malireddi, P. Schreiner, G. Neale, P. Vogel, R. Webby, C. B. Jonsson, T. D. Kanneganti, Synergism of TNF-α and IFN-γ Triggers Inflammatory Cell Death, Tissue Damage, and Mortality in SARS-CoV-2 Infection and Cytokine Shock Syndromes. *Cell* **184**, 149-168.e17 (2021).

15. K. P. Hoefig, A. Reim, C. Gallus, E. H. Wong, G. Behrens, C. Conrad, M. Xu, L. Kifinger, T. Ito-Kureha, K. A. Y. Defourny, A. Geerlof, J. Mautner, S. M. Hauck, D. Baumjohann, R. Feederle, M. Mann, M. Wierer, E. Glasmacher, V. Heissmeyer, Defining the RBPome of primary T helper cells to elucidate higher-order Roquin-mediated mRNA regulation. *Nature Communications 2021 12:1* **12**, 1–18 (2021).

16. J. I. Perez-Perri, B. Rogell, T. Schwarzl, F. Stein, Y. Zhou, M. Rettel, A. Brosig, M. W. Hentze, Discovery of RNA-binding proteins and characterization of their dynamic responses by enhanced RNA interactome capture. *Nature Communications 2018 9:1* **9**, 1–13 (2018).

17. K. Deka, S. Saha, Heat stress induced arginylation of HuR promotes alternative polyadenylation of Hsp70.3 by regulating HuR stability and RNA binding. *Cell Death & Differentiation 2020 28:2* **28**, 730–747 (2020).

18. M. D. Diaz-Muñoz, S. E. Bell, K. Fairfax, E. Monzon-Casanova, A. F. Cunningham, M. Gonzalez-Porta, S. R. Andrews, V. I. Bunik, K. Zarnack, T. Curk, W. A. Heggermont, S. Heymans, G. E. Gibson, D. L. Kontoyiannis, J. Ule, M. Turner, The RNA-binding protein HuR is essential for the B cell antibody response. *Nature Immunology 2015 16:4* **16**, 415–425 (2015).

19. I. C. Osma-Garcia, D. Capitan-Sobrino, M. Mouysset, S. E. Bell, M. Lebeurrier, M. Turner, M. D. Diaz-Muñoz, The RNA-binding protein HuR is required for maintenance of the germinal centre response. *Nat Commun* **12.1** 6556 (2021).

20. J. R. Poganik, M. J. C. Long, M. T. Disare, X. Liu, S. H. Chang, T. Hla, Y. Aye, Post-transcriptional regulation of Nrf2-mRNA by the mRNA-binding proteins HuR and AUF1. *FASEB Journal* **33**, 14636–14652 (2019).

21. C. Tiedje, N. Ronkina, M. Tehrani, S. Dhamija, K. Laass, H. Holtmann, A. Kotlyarov, M. Gaestel, The p38/MK2-Driven Exchange between Tristetraprolin and HuR Regulates AU-Rich Element-Dependent Translation. *PLoS Genet* **8** (2012).

22. F. Salerno, M. Turner, M. C. Wolkers, Dynamic post-transcriptional events governing CD8+ T cell homeostasis and effector function. Trends in immunology, 41(3), 240-254(2020).

23. N. D. Zandhuis, B. P. Nicolet, M. C. Wolkers, RNA-Binding Protein Expression Alters Upon Differentiation of Human B Cells and T Cells. *Front Immunol* **12**, 717324 (2021).

24. A. R. Buxbaum, G. Haimovich, R. H. Singer, In the right place at the right time: visualizing and understanding mRNA localization. *Nature reviews Molecular cell biology*, ***16*.2**, 95-109 (2015).

25. K. Davari, J. Lichti, C. Gallus, F. Greulich, N. H. Uhlenhaut, M. Heinig, C. C. Friedel, E. Glasmacher, Rapid Genome-wide Recruitment of RNA Polymerase II Drives Transcription, Splicing, and Translation Events during T Cell Responses. *Cell Rep* **19**, 643–654 (2017).

26. F. Radford, S. Tyagi, M. L. Gennaro, R. Pine, Y. Bushkin, Flow Cytometric Characterization of Antigen-Specific T Cells Based on RNA and Its Advantages in Detecting Infections and Immunological Disorders. *Critical Reviews™ in Immunology* **36**, 359–378 (2016).

27. A. M. Femino, F. S. Fay, K. Fogarty, R. H. Singer, Visualization of single RNA transcripts in situ. *Science* **280**, 585–590 (1998).

28. A. Raj, P. van den Bogaard, S. A. Rifkin, A. van Oudenaarden, S. Tyagi, Imaging individual mRNA molecules using multiple singly labeled probes. *Nat Methods* **5**, 877–879 (2008).

29. M. Fang, H. Xie, S. K. Dougan, H. Ploegh, A. van Oudenaarden, Stochastic Cytokine Expression Induces Mixed T Helper Cell States. *PLoS Biol* **11**, e1001618 (2013).

30. Y. Bushkin, F. Radford, R. Pine, A. Lardizabal, B. T. Mangura, M. L. Gennaro, S. Tyagi, Profiling T Cell Activation Using Single-Molecule Fluorescence In Situ Hybridization and Flow Cytometry. *The Journal of Immunology* **194**, 836–841 (2015).

31. C. Eliscovich, S. M. Shenoy, R. H. Singer, Imaging mRNA and protein interactions within neurons. *Proc Natl Acad Sci U S A* **114**, E1875–E1884 (2017).

32. F. Mueller, A. Senecal, K. Tantale, H. Marie-Nelly, N. Ly, O. Collin, E. Basyuk, E. Bertrand, X. Darzacq, C. Zimmer, FISH-quant: Automatic counting of transcripts in 3D FISH images. *Nature methods*, ***10*.4**, 277-278 (2013).

33. A. Maekiniemi, R. H. Singer, E. Tutucci, Single molecule mRNA fluorescent in situ hybridization combined with immunofluorescence in S. cerevisiae: Dataset and quantification. *Data Brief* **30**, 105511 (2020).

34. S. van Otterdijk, M. Motealleh, Z. Wang, T. D. Visser, P. Savakis, E. Tutucci, Single-Molecule Fluorescent In Situ Hybridization (smFISH) for RNA Detection in the Fungal Pathogen Candida albicans. *Methods Mol Biol* **2784**, 25–44 (2024).

35. C. Stringer, T. Wang, M. Michaelos, M. Pachitariu, Cellpose: a generalist algorithm for cellular segmentation. *Nature Methods 2020 18:1* **18**, 100–106 (2020).

36. B. P. Nicolet, A. Guislain, M. C. Wolkers, Combined Single-Cell Measurement of Cytokine mRNA and Protein Identifies T Cells with Persistent Effector Function. *The Journal of Immunology* **198**, 962–970 (2017).

37. Q. Han, N. Bagheri, E. M. Bradshaw, D. A. Hafler, D. A. Lauffenburger, J. C. Love, Polyfunctional responses by human T cells result from sequential release of cytokines. *Proc Natl Acad Sci U S A* **109**, 1607–1612 (2012).

38. F. Salerno, A. Guislain, J. J. Freen-Van Heeren, B. P. Nicolet, H. A. Young, M. C. Wolkers, Critical role of post-transcriptional regulation for IFN-γ in tumor-infiltrating T cells. *Oncoimmunology* ***8*.2**, e1532762 (2019).

39. K. Rothamel, S. Arcos, B. Kim, C. Reasoner, S. Lisy, N. Mukherjee, M. Ascano, ELAVL1 primarily couples mRNA stability with the 3′ UTRs of interferon-stimulated genes. *Cell Rep* **35**, 109178 (2021).

40. W. Wang, M. C. Caldwell, S. Lin, H. Furneaux, M. Gorospe, HuR regulates cyclin A and cyclin B1 mRNA stability during cell proliferation. *EMBO J* **19**, 2340–2350 (2000).

41. Y. Akaike, K. Masuda, Y. Kuwano, K. Nishida, K. Kajita, K. Kurokawa, Y. Satake, K. Shoda, I. Imoto, K. Rokutan, HuR Regulates Alternative Splicing of the TRA2β Gene in Human Colon Cancer Cells under Oxidative Stress. *Mol Cell Biol* **34**, 2857–2873 (2014).

42. L. S. Namer, F. Osman, Y. Banai, B. Masquida, R. Jung, R. Kaempfer, An Ancient Pseudoknot in TNF-α Pre-mRNA Activates PKR, Inducing eIF2α Phosphorylation that Potently Enhances Splicing. *Cell Rep* **20**, 188–200 (2017).

43. B. Yang Yang, J.-F. Chang, J. R. Parnes, C. Garrison Fathman. T Cell Receptor (TCR) Engagement Leads to Activation-induced Splicing of Tumor Necrosis Factor (TNF) Nuclear Pre-mRNA. *The Journal of experimental medicine*, ***188*.2**, 247-254 (1998).

44. N. Battich, T. Stoeger, L. Pelkmans, Control of Transcript Variability in Single Mammalian Cells. *Cell* **163**, 1596–1610 (2015).

45. B. C. Mercier, E. Labaronne, D. Cluet, L. Guiguettaz, N. Fontrodona, A. Bicknell, A. Corbin, M. Wencker, F. Aube, L. Modolo, K. Jouravleva, D. Auboeuf, M. J. Moore, E. P. Ricci, Translation-dependent and -independent mRNA decay occur through mutually exclusive pathways defined by ribosome density during T cell activation. *Genome Res* **34**, 394–409 (2024).

46. L. A. Passmore, J. Coller, Roles of mRNA poly(A) tails in regulation of eukaryotic gene expression. *Nature Reviews Molecular Cell Biology 2021 23:2* **23**, 93–106 (2021).

47. W. Dai, G. Zhang, E. V. Makeyev, RNA-binding protein HuR autoregulates its expression by promoting alternative polyadenylation site usage. *Nucleic Acids Res* **40**, 787–800 (2012).

48. J. Cherry, H. Jones, V. A. Karschner, P. H. Pekala, Post-transcriptional Control of CCAAT/Enhancer-binding Protein β (C/EBPβ) Expression: FORMATION OF A NUCLEAR HuR-C/EBPβ mRNA COMPLEX DETERMINES THE AMOUNT OF MESSAGE REACHING THE CYTOSOL. *Journal of Biological Chemistry* **283**, 30812–30820 (2008).

49. W. Zhang, A. C. Vreeland, N. Noy, RNA-binding protein HuR regulates nuclear import of protein. *J Cell Sci* **129**, 4025 (2016).

50. E. L. Van Nostrand, P. Freese, G. A. Pratt, X. Wang, X. Wei, R. Xiao, S. M. Blue, J. Y. Chen, N. A. L. Cody, D. Dominguez, S. Olson, B. Sundararaman, L. Zhan, C. Bazile, L. P. B. Bouvrette, J. Bergalet, M. O. Duff, K. E. Garcia, C. Gelboin-Burkhart, M. Hochman, N. J. Lambert, H. Li, M. P. McGurk, T. B. Nguyen, T. Palden, I. Rabano, S. Sathe, R. Stanton, A. Su, R. Wang, B. A. Yee, B. Zhou, A. L. Louie, S. Aigner, X. D. Fu, E. Lécuyer, C. B. Burge, B. R. Graveley, G. W. Yeo, A large-scale binding and functional map of human RNA-binding proteins. *Nature 2020 583:7818* **583**, 711–719 (2020).

51. E. J. Wherry, S. J. Ha, S. M. Kaech, W. N. Haining, S. Sarkar, V. Kalia, S. Subramaniam, J. N. Blattman, D. L. Barber, R. Ahmed, Molecular Signature of CD8+ T Cell Exhaustion during Chronic Viral Infection. *Immunity* **27**, 670–684 (2007).

52. X. Hu, L. B. Ivashkiv. Cross-regulation of Signaling Pathways by Interferon-γ: Implications for Immune Responses and Autoimmune Diseases. *Immunity*, ***31*.4**, 539-550 (2009).

53. D. I. Jang, A. H. Lee, H. Y. Shin, H. R. Song, J. H. Park, T. B. Kang, S. R. Lee, S. H. Yang. The role of tumor necrosis factor alpha (Tnf-α) in autoimmune disease and current tnf-α inhibitors in therapeutics. *International journal of molecular sciences*, ***22*.5**, 2719 (2021). .

ACKNOWLEDGMENTS

We thank K. Bresser, A.P. Jurgens, and N.D. Zandhuis for critical reading of this manuscript.

Author contribution: Conceptualization, project administration, writing: MVL, MCW, ET. Software, data curation, analysis, visualization: MVL, NS, PS, NK. Validation, investigation, methodology: MVL, BP, AG, AB, LW. Funding acquisition, supervision: MCW.

Competing interests: Authors declare no competing interests.

Funding: This research was supported by the European research council ERC-Printers 817533 (MCW), and by Oncode Institute (MCW).

Data and material availability: Code and scripts have been deposited on github (https://github.com/nikolinasostaric/T-cell_smFISH).

SUPPLEMENTARY MATERIALS:

Materials and Methods

Figs. S1 to S5

Tables S1-S3

References (1-13)

Movie S1-S2

Fig. 1: T-cell smFISH quantification of *IFNG* and *TNF* mRNA in CD8$^+$ T eff cells

A. Schematic workflow of T-cell smFISH. **B.** Maximal projection of smFISH for *IFNG* mRNA (green), *TNF* mRNA (magenta), and DAPI (blue) merged to a single DIC section (grey). Yellow squares indicate *IFNG* and *TNF* transcription sites (TsX). Lower left inset: Gaussian signal of a single mature mRNA. Scale bar: 5 µm **C.** Maximal projection of DAPI (blue), *IFNG* mRNA (top panel), and *TNF* mRNA (bottom panel) in Teff cells re-activated with α-CD3/α-CD28. White arrows: single mRNA molecules. Yellow arrows: TsX. Scale bar: 5 µm. **D.** Number of nascent *IFNG* (left) and *TNF* (right) RNA per TsX. Each dot depicts one transcription site. Data pooled from 3 donors. n ≥ 1000 cells/time point. Red bar: median. **E.** Number of mature *IFNG* (left) and *TNF* (right) mRNA in Teff cells expressing ≥1 mature mRNA. Each dot represents an individual cell. Data pooled from 3 donors. **F.** Cytokine expression measured by intracellular cytokine staining. Bref A was added for max. 2h. Left panels: representative flow cytometry plot. Right panels: n=3 donors, line= mean. **G.** Violin plot of protein fluorescence intensity per cell. Data pooled from 3 donors. Red bar: median.

Fig. 2: Cytokine mRNA and protein expression is dominated by double expressors

A. Number of nascent *IFNG* (left) and *TNF* (right) RNA per TsX in single positive (SP, blue) or double positive (DP, orange) expressors upon T cell activation. Each dot represents an individual cell, data pooled from 3 donors. Red bar: median. **B.** Percentage of Teff cells expressing ≥1 mature *IFNG* (left) and *TNF* (right) mRNA in single and double positive mRNA expressors. n=3 donors, line: mean. **C.** Number of mature *IFNG* (left panel) and *TNF* (right panel) mRNA SP and DP expressors containing ≥1 mRNA. Each dot represents an individual cell. Data pooled from 3 donors. Red bar: median. **D.** Violin plot of protein fluorescence intensity of cytokine production in SP and DP producers per cell. Data pooled from 3 donors. Red bar: median. *p≤0.05, **p≤0.01, ***p≤0.001, ****p≤0.0001 ns: non-significant. Kruskal-Wallis non-parametric test, and post-hoc Tukey HSD test for comparing time points.

Fig. 3: *IFNG* and *TNF* mRNA localization and translation control

A. Ratio of cytoplasmic mRNA versus nuclear mRNA per cell of Teff cells expressing ≥1 mature mRNA. Data represented as pseudo-log10 transformed. Dotted line represents equal distribution in nucleus and cytoplasm. n ≥ 500 cells/time point, pooled from 3 donors. Red bar:

median. **B.** Left: Experimental setup of transcription/translation block in Teff cells. Right: MAX projections of T-cell smFISH. Scale bar; 5µm. **C.** Number of nascent *IFNG* (left) and *TNF* (right) RNA per TsX. Each dot represents an individual cell. n ≥ 1000 cells/condition, one donor. Red bar: median. **D.** Mature cytokine mRNA of Teff cells expressing ≥1 mature mRNA. **E.** Number of nuclear (N, black) and cytoplasmic (C, grey) cytokine mRNA. **F.** Cytokine mRNA expression measured by qRT-PCR upon treatment with ActD, or ActD and Harr combined, normalized to control (Ctrl). n=3 donors, mean ± SD.

Fig. 4: IFNG and TNF mRNA and protein expression HuR-KO Teff cells

A. Percentage of cytokine-producing Ctrl (C) and HuR-KO Teff cells (KO). BrefA was added at 0h. n=3 donors. **B.** Violin plot of protein fluorescence intensity per cell, from 3 pooled donors. Red bar: median **C.** Control (top panel) and HuR KO (bottom panel) Teff cells were activated with α-CD3/α-CD28. MAX projection of T-cell smFISH. Scale bar: 5µm. **D.** Number of mature cytokine mRNA in Teff cells expressing ≥1 mature mRNA. n ≥ 1500 cells/time point, from 3 pooled donors. Red bar: median. **E.** Number of nascent cytokine RNA per TsX. Red bar: median. *p≤0.05, **p≤0.01, ***p≤0.001, ****p≤0.0001 ns: non-significant. Kruskal-Wallis non-parametric test, and post-hoc Tukey HSD test for comparing time points.

Fig. 5: *IFNG* and *TNF* mRNA localization and PTR in HuR-del Teff cells

A. Number of cytoplasmic (top) and nuclear (bottom) cytokine mRNAs in control (Ctrl) or HuR-KO (KO) Teff cells that express ≥1 mature mRNA per cell. Data represented as pseudo-log10 transformed, with a coefficient of 0.5 added. Each dot represents an individual cell, data pooled from 3 donors. Red bar: median **B.** Ratio of cytoplasmic mRNA versus nuclear mRNA in Ctrl or HuR-KO Teff cells expressing ≥1 mature mRNA per cell. Data represented as pseudo-log10 transformed. Data from 3 pooled donors. Red bar: median **C.** Left: *IFNG* and *TNF* mRNA expression determined by qRT-PCR in Ctrl or HuR-KO Teff cells activated for 1h with α-CD3/α-CD28. Right *IFNG* and *TNF* mRNA levels in Teff upon ActD treatment. Cytokine mRNA expression at 1h of T cell activation is considered 100%. (n=3 donors, mean ± SD). **D.** Measurement of poly(A) length of cytokine mRNA using RL-PAT in control (Ctrl) or HuR-KO (KO) Teff cells activated for 1h with α-CD3/α-CD28 using the RL-PAT assay. Arrows indicate *IFNG* 3'UTR full-length: 812bp and *TNF* 3'UTR full-length: 609bp.

Fig. 1

Lattanzio et. al

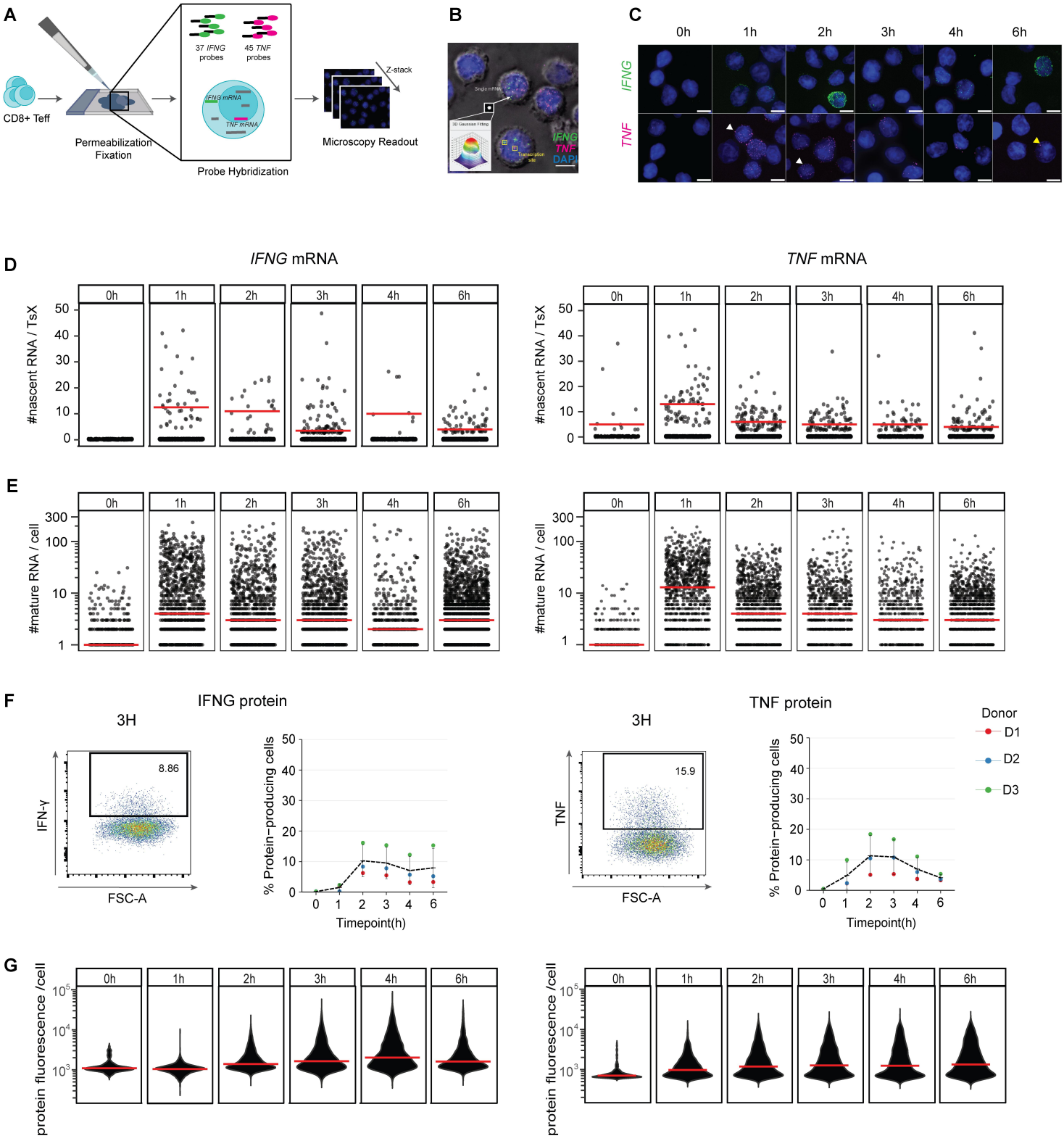

Fig.2 **Lattanzio et al.**

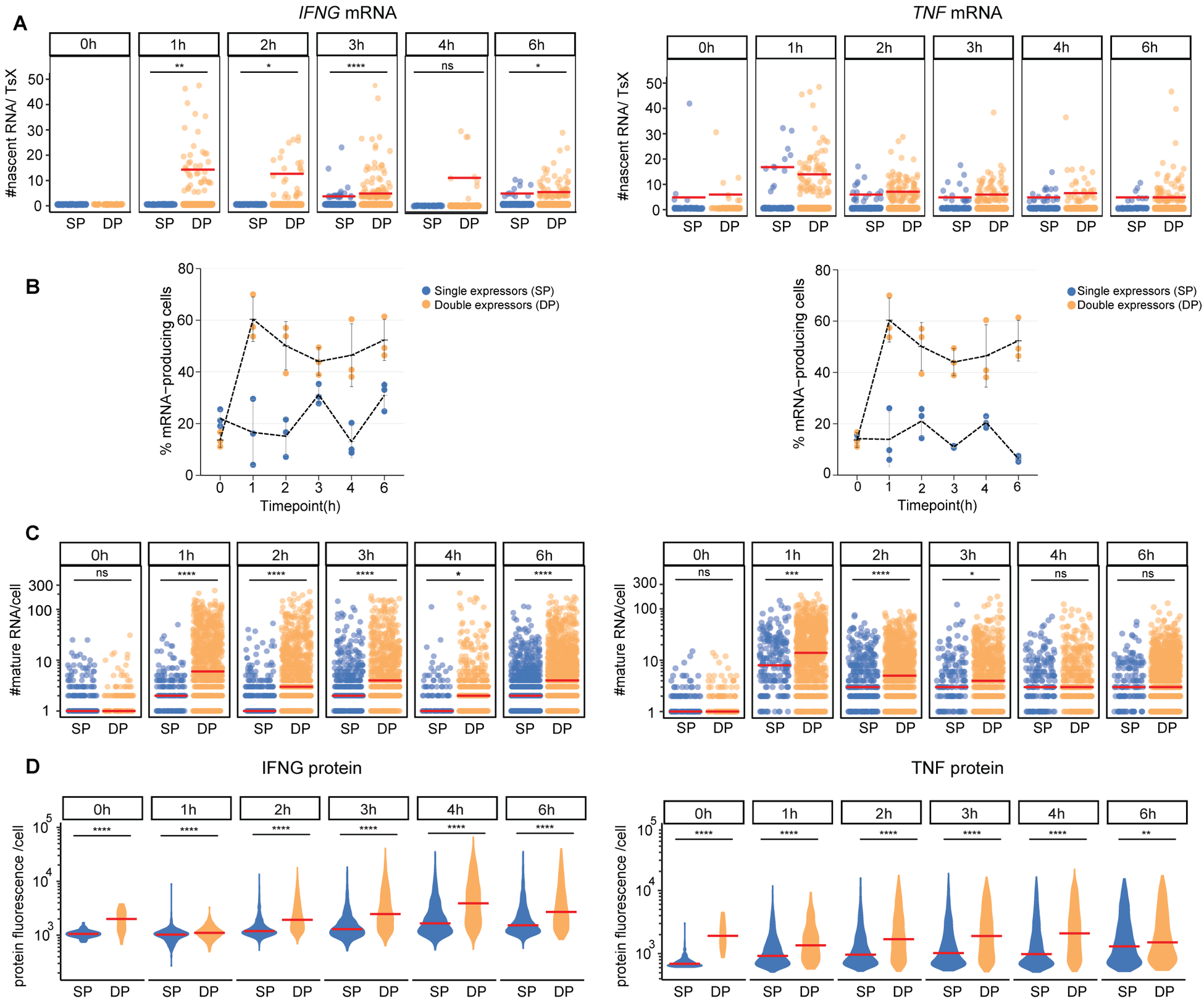

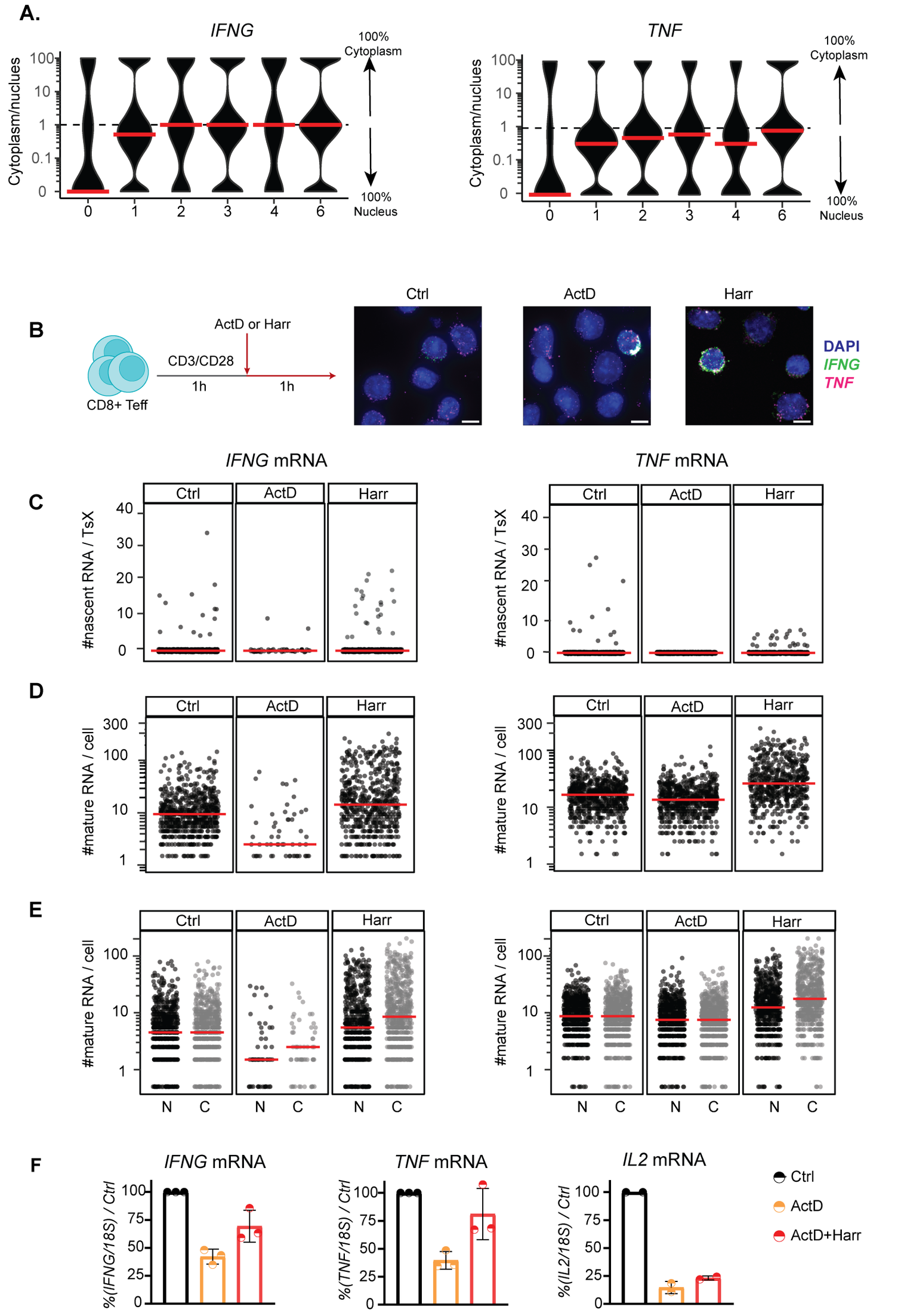
A.
IFNG
TNF
Cytoplasm/nuclues
100
10
1
0.1
0
0
1
2
3
4
6
100% Cytoplasm
100% Nucleus
B
CD8+ Teff
CD3/CD28
ActD or Harr
1h
1h
Ctrl
ActD
Harr
DAPI
IFNG
TNF
C
IFNG mRNA
TNF mRNA
#nascent RNA / TsX
Ctrl
ActD
Harr
D
#mature RNA / cell
E
#mature RNA / cell
N
C
F
IFNG mRNA
TNF mRNA
IL2 mRNA
%(IFNG/18S) / Ctrl
%(TNF/18S) / Ctrl
%(IL2/18S) / Ctrl
Ctrl
ActD
ActD+Harr

Fig.4

Lattanzio et al.

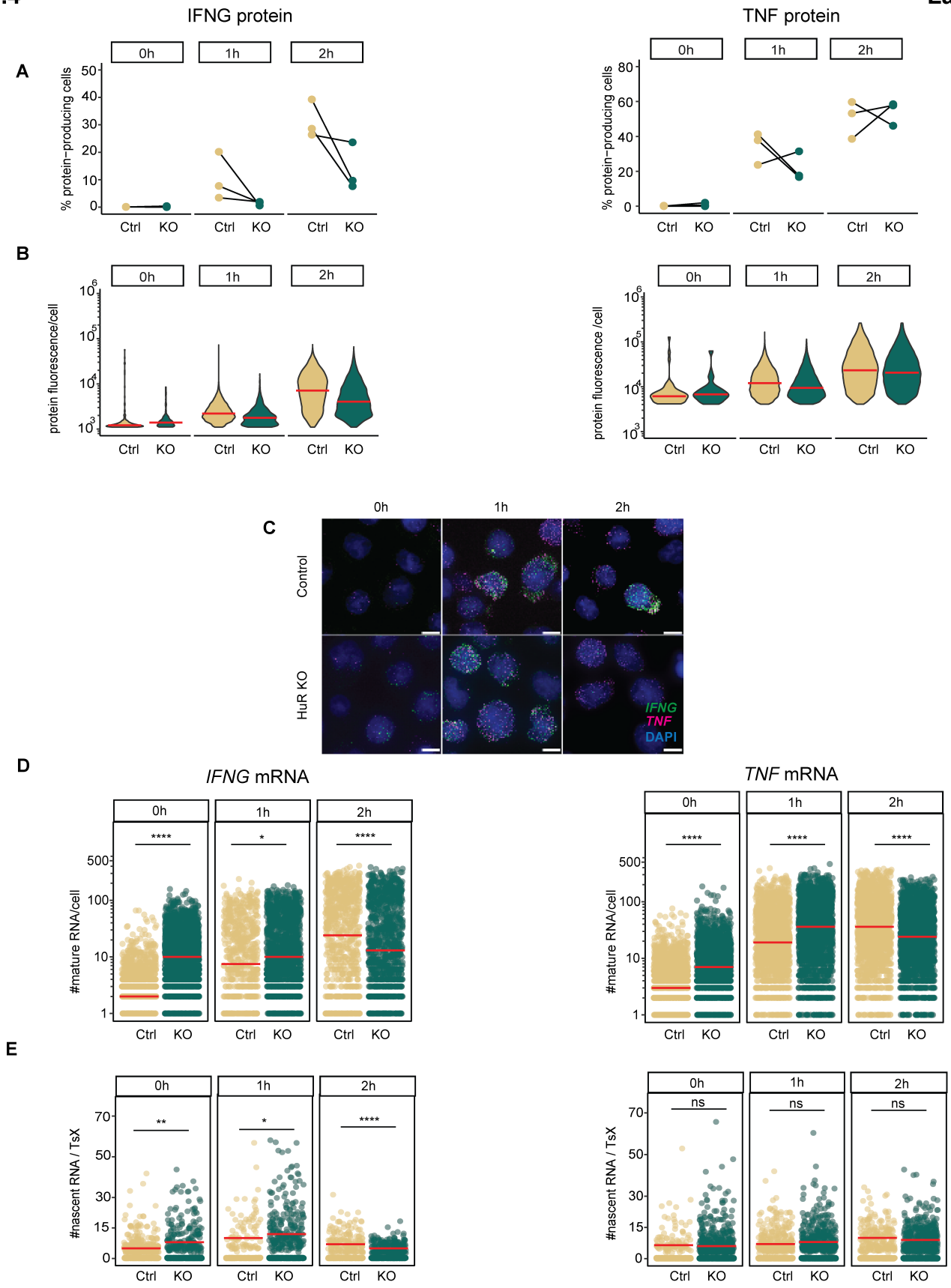
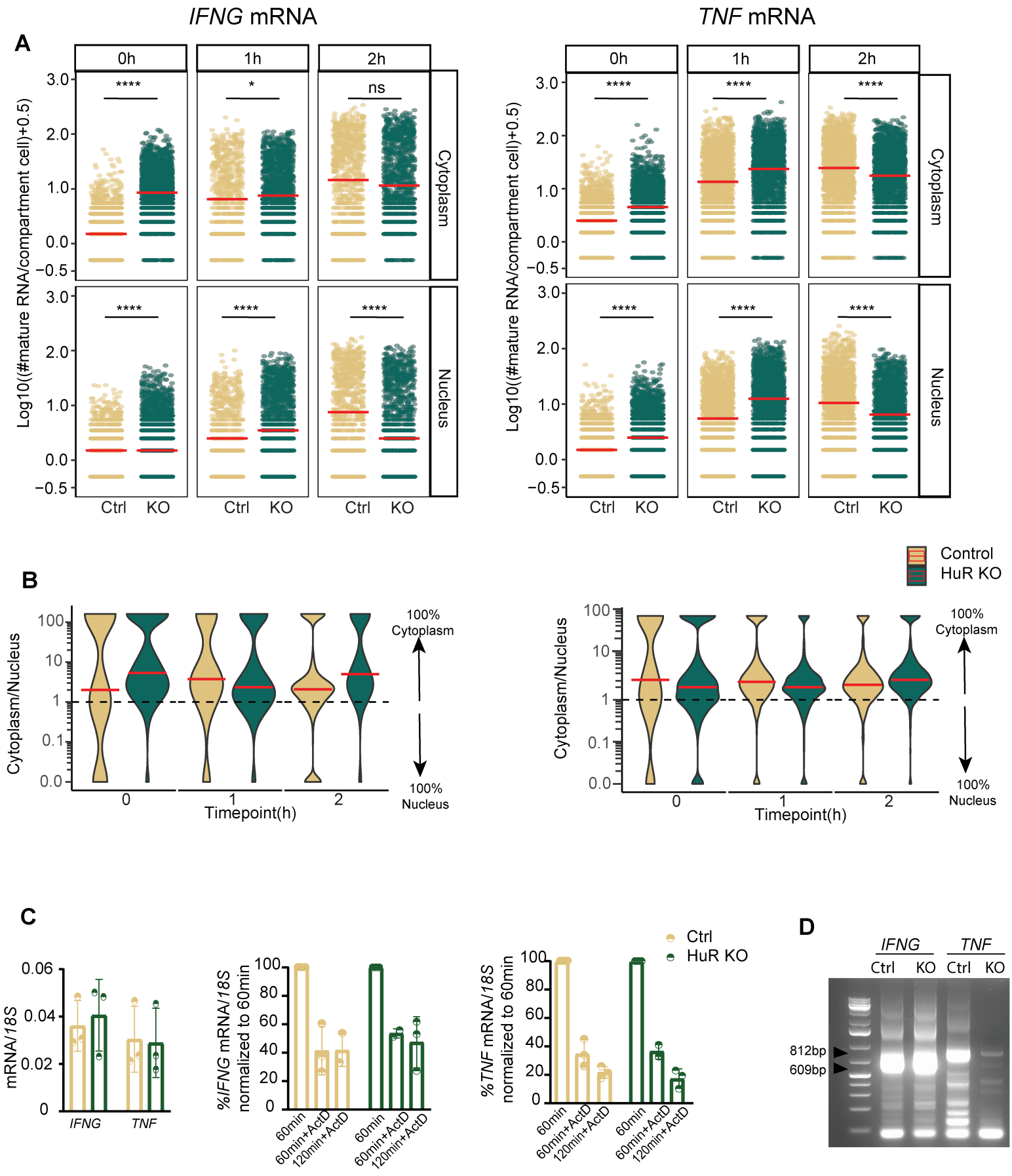
Fig.5 **Lattanzio et al.**